applied sciences

MDPI

Article

Robust Control Examples Applied to a Wind Turbine Simulated Model

Silvio Simani [1,*] and Paolo Castaldi [2]

[1] Dipartimento di Ingegneria, Università degli Studi di Ferrara, Via Saragat 1E, 44122 Ferrara, Italy
[2] Dipartimento di Ingegneria dell'Energia Elettrica e dell'Informazione "Guglielmo Marconi"—DEI, Alma Mater Studiorum Università di Bologna, Viale Risorgimento 2, 40136 Bologna, Italy; paolo.castaldi@unibo.it
* Correspondence: silvio.simani@unife.it; Tel.: +39-053-297-4844

Received: 25 November 2017; Accepted: 19 December 2017; Published: 26 December 2017

Abstract: Wind turbine plants are complex dynamic and uncertain processes driven by stochastic inputs and disturbances, as well as different loads represented by gyroscopic, centrifugal and gravitational forces. Moreover, as their aerodynamic models are nonlinear, both modeling and control become challenging problems. On the one hand, high-fidelity simulators should contain different parameters and variables in order to accurately describe the main dynamic system behavior. Therefore, the development of modeling and control for wind turbine systems should consider these complexity aspects. On the other hand, these control solutions have to include the main wind turbine dynamic characteristics without becoming too complicated. The main point of this paper is thus to provide two practical examples of the development of robust control strategies when applied to a simulated wind turbine plant. Extended simulations with the wind turbine benchmark model and the Monte Carlo tool represent the instruments for assessing the robustness and reliability aspects of the developed control methodologies when the model-reality mismatch and measurement errors are also considered. Advantages and drawbacks of these regulation methods are also highlighted with respect to different control strategies via proper performance metrics.

Keywords: wind turbine simulator; data-driven and model-based approaches; fuzzy identification; on-line estimation; robustness and reliability

1. Introduction

Wind turbine plants represent complex and nonlinear dynamic systems usually driven by stochastic inputs and different disturbances describing gravitational, centrifugal and gyroscopic loads. Moreover, their aerodynamic models are uncertain and nonlinear, whilst wind turbine rotors are subject to complex turbulent wind fields, especially in large systems, thus yielding to extreme fatigue loading conditions. In this way, the development of viable, robust and reliable control solutions for wind turbines can become a challenging issue [1,2].

Usually, a model-based control design requires an accurate description of the system under investigation, which has to include different parameters and variables in order to model the most important nonlinear and dynamic aspects. Moreover, the wind turbine working conditions can produce further problems for the design of the control method. In general, commercial codes are not able to adequately describe the wind turbine overall dynamic behavior; usually, special simulation software solutions are used. On the other hand, control schemes have to manage the most important turbine dynamics, without being too complex and unwieldy. Control methods for wind turbines usually rely on the signals from sensors and actuators, with a system that connects these elements together. Hardware or software modules elaborate these signals to generate the output signals for actuators. The main feature of the control law consists of maintaining safe and reliable

working conditions of the wind turbine, while achieving prescribed control performances and allowing for optimal energy conversion, as shown, e.g., in recent works applied to the same wind turbine model considered in this work [3].

Today's wind turbines can implement several control strategies to allow for the required performances. Some turbines use passive control methods, such as in fixed-pitch, stall control machines. In this case, the system is designed so that the power is limited above rated wind speed through the blade stall. Therefore, the control of the blades is not required [1]. In this case, the rotational speed control is proposed, thus avoiding the inaccuracy of measuring the wind speed. Rotors with pitch regulation are usually used for constant-speed plants, in order to provide a power control that works better than the blade stall solution. In these machines, the blade pitching is controlled in order to provide optimal power conversion with respect to modeling errors, wind gusts and disturbance. However, when the system works at constant speed and below rated wind speed, the optimal conversion rate cannot be obtained. Therefore, in order to maximize the power conversion rate, the rotational speed of the turbine must vary with wind speed. Blade pitch control is thus used also above the rated wind speed [1]. A different control method can introduce the yaw regulation to orient the machine into the wind field. A yaw error reference from a nacelle-mounted wind direction sensor system must be included in order to calculate this reference signal [4].

Regarding the regulation strategies proposed in this paper, two control design examples are described and applied to a wind turbine system. The wind turbine model exploited in this work is freely available for the MATLAB® and Simulink® environments, and already proposed as benchmark for an international competition regarding the validation of fault diagnosis and fault tolerant control approaches [3].

In particular, a first data-driven method relying on a fuzzy identification approach to the control design is considered. In fact, since the wind turbine mathematical model is nonlinear with uncertain inputs, fuzzy modeling represents an alternative tool for obtaining the mathematical description of the controlled process. In contrast to purely nonlinear identification schemes (see, e.g., [5]), fuzzy modeling and identification methods are able to directly provide nonlinear models from the measured input-output signals. Therefore, this paper suggests to model the wind turbine plant via Takagi–Sugeno (TS) fuzzy prototypes [6], whose parameters are obtained by identification procedures. This approach is also motivated by previous works by the same authors [7]. On the other hand, concerning the control design, the paper proposes also a fuzzy control method for the regulation of the blade pitch angle, and the generator torque of the wind turbine system.

With respect to similar works (see, e.g., [8]), this paper suggests an off-line identification approach, without any on-line optimization schemes, thus enhancing real-time implementations. Note also that the works by the same authors (see, e.g., [9]), addressed a different design procedure of the fuzzy regulator, that consists of fuzzy PI controllers. On the other hand, this paper proposes the direct estimation of the fuzzy regulator by means of an identification scheme.

Regarding the second model-based strategy presented in this paper, it relies on an adaptive control scheme [10]. Again, with respect to pure nonlinear control methods [11], it does not require a detailed knowledge about the model structure. Therefore, this work suggests the implementation of controllers based on adaptive schemes, used for the recursive derivation of the controller model. In particular, a recursive Frisch scheme extended to the adaptive case for control design is considered in this study, as proposed, e.g., in [9] by the same authors, which makes use of exponential forgetting laws. This allows the on-line application of the Frisch scheme to derive the parameters of a time-varying controller.

Since it is necessary to evaluate the robustness and the reliability of the designed control methods with respect to modeling uncertainties, disturbance, and measurement errors, the verification and validation tools use extensive Monte Carlo simulations. In fact, the wind turbine system contains elements that cannot be described by analytical models. Thus, the Monte Carlo analysis represents a solution for testing the robustness and reliability features of the control schemes when applied to the

wind turbine model. This paper compares the proposed methodologies also with respect to different control methods based on sliding mode techniques, neural controllers, or gain scheduling methods. However, with respect again to [9] by the same authors, different comparisons are proposed in this work that exploit proper performance metrics.

It is worth highlighting the main features of the proposed data-drive and model-based approaches. Indeed, the term "model-based" could be misleading in this case. In fact, the adaptive control approach suggested in this work should be considered as "active" control method, instead. In fact, the control design relies on an identified model of the process under investigation. In this way, the parameters of the process model are identified on-line via a recursive estimation procedure, in order to adapt this identified model with respect to both the different operating conditions and possible process uncertainty. Due to this adaptation scheme, the control design technique is able to achieve robustness characteristics with respect to possible uncertainty and disturbance effects. On the other hand, the proposed on-line control scheme can be applied to nonlinear dynamic processes, due to its capabilities to recursively track the changes of the controlled process. Moreover, the adaptive control law can be designed by means of different rules that are functions of the process model parameters, thus making the control design solutions robust with respect to disturbances. Another key aspect concerns the identification method exploited for estimating the model parameters. The proposed approach relies on an Error-In-Variable (EIV) scheme [12], which is more general and less conservative than standard identification techniques. For example, the classical Least Square Method (LSM) assumes that only the output is possibly affected by uncertainty (noise) [13]. Therefore, the EIV identification scheme proposed in this work for the estimation of the controller parameters makes the developed solutions much more robust and reliable than standard control schemes. Finally, with respect to standard PID regulators, which can be seen as 'passive' control solutions, they are not able to track the changes of the controlled process, since their parameters are usually optimized on the basis on the nominal process model [14].

Finally, this work is organized as follows. Section 2 recalls the wind turbine model considered for control design purposes. Section 3 addresses the data-driven scheme exploited for the derivation of the fuzzy controller, proposed in Section 3.1. On the other hand, the model-based control design is considered in Section 3.2, based on its mathematical derivation also described in Section 3. The achieved results and comparisons with different control strategies are outlined in Section 4. The robustness and reliability features of the developed control strategies are also investigated. Finally, Section 5 ends the paper by summarizing the main achievements of the work.

2. Wind Turbine Simulated Model

Today's wind turbines contribute to a larger and larger part of the world's power production. At the same time the size of the standard turbine has been increasing, as well. Turbines in the megawatt size, as most often installed at present, are expensive, and hence the reliability of their control techniques represents an important issue. They should be able to produce as much time as possible. A way to contribute to ensure this consists in introducing advanced control systems on the wind turbines. The state-of-the-art of advanced control schemes for industrial wind turbines shows that they are quite simple and often conservative [15]. For example, turbines deployments are turn off even at earlier malfunctions, to wait for service. Consequently, the use of advanced control schemes could improve the on-time of the turbine, even though that might result in production with limited power for some anomalous working conditions [15]. Some works on advanced control solutions for wind turbines were proposed. For example, an observer based scheme applied to the pitch system was presented in [16]. On the other hand, priority relation based scheme for change detection was presented in [17], whilst an unknown input observer applied to the wind turbine drive train in [18]. Furthermore, the wind turbine electrical conversion system was investigated in [19–21]. Therefore, in general, it would be beneficial to compare different control schemes for wind turbine application in order to find the best solutions, as considered in this paper. However, since

a wind turbine is a large and complex system such a comparison can only be performed on a limited set of situations. Therefore, in order to test different advanced control techniques for wind turbine applications, this paper considered the benchmark model of a wind turbine process on system level, containing sensors, actuators and systems typical of an energy conversion plant. This benchmark model describes a realistic generic three-bladed horizontal variable speed wind turbine with a full converter coupling, formerly proposed in [22]. This generic turbine has a rated power of 4.8 MW. Since this model works on a system level, the fast control loops of the converters are not considered. Moreover, since it is a model on system level, its converter and pitch system models are simplified, because they are controlled by internal governors working at higher frequencies than the system model.

This section outlines the wind turbine model, whose sampled inputs and outputs will be used for the proposed control designs, as shown in Section 3. More details concerning the accurate derivation of the simulator model can be found in preliminary works [23,24] and definitely presented in [22]. In fact, this simulator was proposed for an international competition regarding fault diagnosis and fault tolerant control techniques started in 2009, whose results were summarized in [3,25].

The wind turbine system exploited in this work uses a nonlinear dynamic model representing the wind acting on the wind turbine blades, thus producing the movement of the low-speed rotor shaft. The higher speed required by the electric converter is produced by means of a gear box. The simulator is described in more detail, e.g., in [22,25]. A scheme of the wind turbine simulator considered in this paper is represented in Figure 1 with its main blocks.

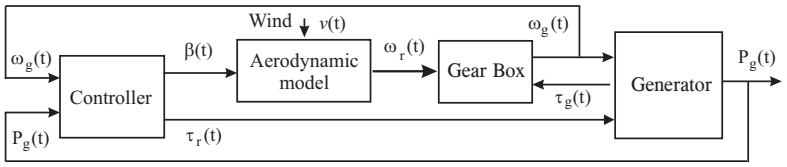

Figure 1. Scheme of the wind turbine process.

Both the generator speed ω_g and the generator power P_g are controller by means of the two control inputs representing the generator torque $\tau_g(t)$ and the blade pitch angle $\beta(t)$. Several signals can be acquired from the wind turbine simulator. In particular, the main signals available from the wind turbine simulator and used for control purpose are listed in the following:

β: blade pitch angle (deg);
ω_g: generator/converter speed (rad/s);
P_g: generator power P_g (W);
ω_r: rotor speed (rad/s);
τ_r: requested torque (N m);
τ_g: generator torque (N m);
τ_{aero}: aerodynamic torque (N m);
v: wind speed (m/s);

The aerodynamic model defining the aerodynamic torque provides the $\tau_{aero}(t)$ signal, which is a nonlinear function of the wind speed $v(t)$, and it is not highlighted in Figure 1 since included in the 'Aerodynamic model' block. This measurement is very difficult to be acquired correctly, as described in [25].

The aerodynamic model reported in Figure 1 is described by the following relation:

$$\tau_{aero}(t) = C_p\left(\beta_r(t),\, \lambda(t)\right) \frac{\rho\, A\, v^3(t)}{2\,\omega_r(t)} \tag{1}$$

where the variable ρ represents the air density, whilst A is the effective rotor area.

The pitch system implemented in the wind turbine benchmark as depicted in Figure 1 uses a second-order transfer function, represented by Equation (2):

$$\frac{\beta_r(s)}{\beta(s)} = \frac{\omega_n^2}{s^2 + 2\,\chi\,\omega_n\,s + \omega_n^2} \tag{2}$$

where β_r is the actuated pitch angle, which is exploited in Equation (1), whilst β is the controlled pitch angle. ω_n is the natural frequency of the pitch actuator model, and χ its damping ratio.

Another important variable is represented by the so-called tip-speed ratio, which is defined as:

$$\lambda(t) = \frac{\omega_r(t)\,R}{v(t)} \tag{3}$$

with R the rotor radius. $C_p(\cdot)$ represents the power coefficient, that is normally represented via a two-dimensional map [25]. The expression of Equation (1) allows the computation of the signal $\tau_{aero}(t)$ (highlighted in Figure 1) by means of the estimated wind speed $v(t)$ and the signals $\beta(t)$ and $\omega_r(t)$. Due to the uncertainty of the wind speed, the estimate of $\tau_{aero}(t)$ is considered affected by an unknown measurement error, which justifies the robust approaches described in Section 3. Moreover, the nonlinearity represented by the expressions of Equations (1) and (3) motivates the required reliable and robust control approaches suggested in this work.

The wind turbine simulator includes a two-mass model that is exploited to describe the drive-train system depicted in Figure 1, as shown by the following linear state-space representation [22]:

$$\begin{bmatrix} \dot{\omega}_r(t) \\ \dot{\omega}_g(t) \\ \dot{\theta}_\Delta(t) \end{bmatrix} = \mathrm{A}_{dt} \begin{bmatrix} \omega_r(t) \\ \omega_g(t) \\ \theta_\Delta(t) \end{bmatrix} + \mathrm{B}_{dt} \begin{bmatrix} \tau_{aero}(t) \\ \tau_g(t) \end{bmatrix} \tag{4}$$

where the matrices A_{dt} and B_{dt} are defined as:

$$\mathrm{A}_{dt} = \begin{bmatrix} -\frac{B_{dt}-B_r}{J_r} & \frac{B_{dt}}{N_g\,J_r} & -\frac{K_{dt}}{J_r} \\ \frac{\eta_{dt}\,B_{dt}}{N_g\,J_g} & \frac{-\frac{\eta_{dt}\,B_{dt}}{N_g^2}-B_g}{J_g} & \frac{\eta_{dt}\,K_{dt}}{N_g\,J_g} \\ 1 & -\frac{1}{N_g} & 0 \end{bmatrix} \tag{5}$$

and:

$$\mathrm{B}_{dt} = \begin{bmatrix} -\frac{1}{J_r} & 0 \\ 0 & -\frac{1}{J_g} \\ 0 & 0 \end{bmatrix} \tag{6}$$

where J_r is the momentum of inertia of rotor shaft, K_{dt} is the torsion stiffness of the drive-train, B_{dt} is the torsion damping coefficient of the drive-train, B_g is the viscous friction of the generator shaft, N_g is the gear ratio, J_g is the moment of inertia of the generator shaft, η_{dt} is the efficiency of the drive-train, and θ_Δ is the torsion angle of the drive train. Note that the benchmark simulator considered in this work does not include possible nonlinear gearbox dynamics, as addressed e.g., in [26–28]. However, the data-driven approach proposed in this study could be able to include this further nonlinearity for the design of the control solutions.

Moreover, the generator/converter dynamics are described as a first-order transfer function, as highlighted by Equation (7):

$$\frac{\tau_g(s)}{\tau_r(s)} = \frac{\alpha_{gc}}{s + \alpha_{gc}} \tag{7}$$

s being the Laplace operator, $1/\alpha_{gc}$ is the time constant of the generator/converter, whilst the power P_g produced by the generator is given by Equation (8):

$$P_g(t) = \eta_g \, \omega_g \, \tau_g(t) \tag{8}$$

with η_g denoting the efficiency of the generator. More details regarding the considered simulator are in [25].

Under these assumptions, the complete state-space description of the wind turbine model has the form of Equation (9):

$$\begin{cases} \dot{x}_c(t) &= f_c\left(x_c(t), u(t)\right) \\ y(t) &= x_c(t) \end{cases} \tag{9}$$

where $u(t) = \left[\beta(t),\, \tau_g(t)\right]^T$, $y(t) = \left[P_g(t),\, \omega_g(t)\right]^T$, and $x_c(t) = \left[P_g(t),\, \omega_g(t)\right]^T$ are the control inputs, the monitored output measurements, and the state vector, respectively, as shown in Figure 1. $P_g(t)$ is the generator power measurement, whilst $f_c\left(\cdot\right)$ represents the continuous-time nonlinear function that will be approximated via discrete-time models from N sampled data u_k and y_k, with the sample index $k = 1, 2, \ldots N$, as presented in Section 3. The model parameters, and the map $C_p\left(\beta, \lambda\right)$ are chosen in order to represent a realistic wind turbine plant [25].

Note that Section 4.2 will analyze the reliability and robustness properties of the developed controllers when parameter variations and measurement errors are considered. This investigation will rely on the Monte Carlo tool, since the control behavior and the tracking capabilities depend on both the model-reality mismatch effects and the input-output uncertainty levels. Therefore, this analysis will be performed by describing the parameters of the wind turbine model simulator as Gaussian stochastic processes with average values corresponding to the nominal ones summarized in Table 1 [25].

Table 1. Wind turbine benchmark parameters.

Variable	R	χ	ω_n	B_{dt}	B_r
Nominal value	57.5 m	0.6	11.11 rad s^{-1}	775.49 N m s rad^{-1}	7.11 N m s rad^{-1}
Variable	B_g	K_{dt}	η_{dt}	J_g	J_r
Nominal value	45.6 N m s rad^{-1}	$2.7 \cdot 10^9$ N m rad^{-1}	0.97	390 kg m^2	$55 \cdot 10^6$ kg m^2

Moreover, the input and output measurements available from the wind turbine simulator are assumed to be acquired via sensors [25] that introduce additive Gaussian noise processes with zero mean and standard deviation values summarized in Table 2.

Table 2. Sensor standard deviation values used in the wind turbine simulator [25].

Variable	$v(t)$	ω_r	ω_g	τ_g	P_g	β
Std. Dev. Value	0.5 m/s	0.025 rad/s	0.05 rad/s	90 Nm	10^3 W	0.2 deg

Note that the parameters summarized in Table 2 are the values implemented in the wind turbine benchmark simulator that has been used in this work for the validation of the proposed control solutions. These values represent the uncertainty and disturbance effects of a realistic wind turbine deployment, as modeled by the wind turbine benchmark simulator presented and developed in [25].

On the other hand, this benchmark model set-up uses a predefined wind speed sequence $v(t)$ consisting of real measured wind data of a wind park from 0 to 4400 s. Figure 2 highlights that this wind speed covers the range from 5 to 20 m/s, with a few spikes at 25 m/s, which is a good coverage of normal operational for a wind turbine.

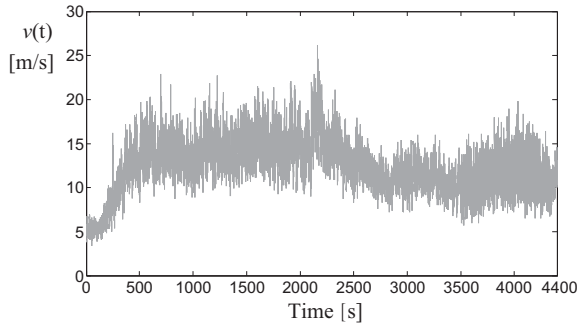

Figure 2. The wind speed sequence $v(t)$ used in the benchmark model.

It is worth noting also that the nonlinearity represented by Equations (1) and (3) is sketched in Figure 3, for different values of $\lambda(t)$ (i.e., $v(t)$) and $\beta(t)$.

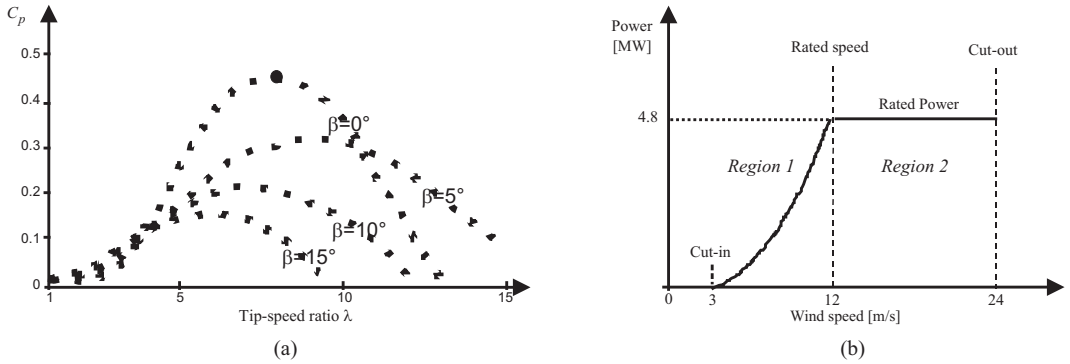

Figure 3. Examples of power coefficient function (**a**) and power curve (**b**).

Figure 3 also shows the power curve that highlights the the so-called partial load (Region 1) and full load (Region 2) working conditions of a wind turbine [22]. In fact, the baseline controller implemented in the wind turbine simulator works in these two operating conditions. A schematic diagram of the baseline wind turbine controller system is detailed in Figure 4.

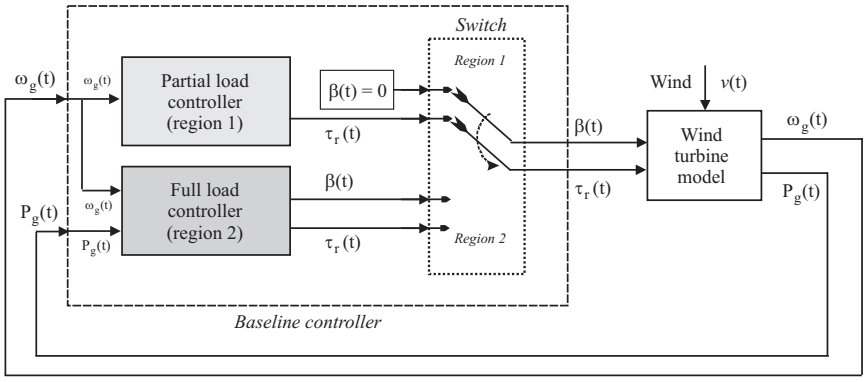

Figure 4. The details of the baseline wind turbine controller.

In particular, Figure 4 highlights that in partial load working condition, the optimal tracking is achieved without any pitching of the blades, which are fixed to zero degrees. In this case, λ is constant at its optimal value λ_{opt}, that is defined by the maximal value of the power coefficient map C_p when $\beta = 0$ degrees, as shown in Figure 3a. Therefore, this working condition is completely defined by setting $\tau_g = \tau_r$ (i.e., the generator torque is equal to the required reference value) with pitch angle $\beta = 0$ degrees.

The reference torque signal τ_r shown in Figure 1 is computed as:

$$\tau_r = K_{opt}\,\omega_g^2 \tag{10}$$

where:

$$K_{opt} = \frac{1}{2}\,\rho\,A\,R^3\,\frac{C_{p_{\max}}}{\lambda_{opt}^3} \tag{11}$$

with $C_{p_{\max}}$ the maximal value of C_p, related the to λ_{opt}, i.e., the optimal tip-speed ratio, as sketched in Figure 3a.

When the power reference $P_r = 4.8$ MW is achieved by the wind turbine system (it corresponds to the so-called rated power) [22], and the wind speed $v(t)$ increases, the controller is switched to the control Region 2 (full load condition). In this working condition (Region 2), the control objective consists of tracking the power reference P_r, obtained by regulating β, such that the C_p is decreased, as shown in Figure 3a. In a traditional industrial control scheme, usually a PI controller is used to keep ω_g at the prescribed value by changing β; the second input of the controller is τ_g.

The baseline controller considered in this work was implemented with a sample frequency at 100 Hz, i.e., $T_s = 0.01$ s. In full load conditions, i.e., in Region 2, the actuated input β is controlled via the relations of Equation (12) [25]:

$$\begin{cases} \beta_k &= \beta_{k-1} + k_p\,e_k + \left(k_i\,T_s - k_p\right)\,e_{k-1} \\ e_k &= \omega_{g_k} - \omega_{nom} \end{cases} \tag{12}$$

with the sample index $k = 1, 2, \ldots, N$. The parameters for this PI speed controller are $k_i = 0.5$ (1/s) and $k_p = 3$ (deg/rad/s), with sampling time $T_s = 0.01$ s, as reported in [25]. For the case of the wind turbine system considered in this paper, with rated power $P_r = 4.8$ MW, the constant ω_{nom} is equal to 162 (rad/s) [22].

The control of the further input τ_g shown in Figure 1, a second PI regulator is used, in the form of Equation (13):

$$\begin{cases} \tau_{rk} &= \tau_{rk-1} + k_p\,e_k + \left(k_i\,T_s - k_p\right)\,e_{k-1} \\ e_k &= P_{g_k} - P_r \end{cases} \tag{13}$$

The parameters for this second PI power controller are $k_i = 0.014$ and $k_p = 447 \times 10^{-6}$ [25].

Finally, note that in Region 2 (partial load, below the rated wind speed) the wind turbine is regulated only by means of the torque input $\tau_g(t)$. In this situation, the blade pitching system is not exploited to achieve the optimal power conversion, as highlighted in Figure 4. On the other hand, in Region 2 (full load, above the rated wind speed), the wind turbine control regulates both the blade pitch angle $\beta(t)$ and the control torque $\tau_g(t)$. The wind turbine Simulink® model considered in this work includes also saturation blocks that limit the values of the control signals, which were not reported in Figures 1 and 4.

3. Data-Driven and Model-Based Control Designs

This section describes the two approaches considered in this paper for obtaining the control laws by using data-driven and model-based methodologies. Once a suitable mathematical description of the monitored process is provided, the derivation of the controller structure is sketched in Section 3.1 for the fuzzy approach, whilst Section 3.2 proposes a different method relying on an adaptive technique.

The first method proposed in this paper for the derivation of the wind turbine controller is based on a fuzzy clustering technique to partition the available data into subsets characterized by linear behaviors. The integration between clusters and linear regression is exploited, thus allowing for the combination of fuzzy logic techniques with system identification methodologies. These tools are already available and implemented in the MATLAB® Fuzzy Modeling and IDentification (FMID) Toolbox recalled below [6]. This study proposes the use of TS fuzzy prototypes since they are able to

model nonlinear dynamic systems with arbitrary accuracy [6]. The switching between the local affine submodels is achieved through a smooth function of the system state defined exploiting the fuzzy set theory and its tools.

In more detail, the fuzzy estimation scheme relies on a two-step algorithm, in which, the working regions are first defined by exploiting the data fuzzy clustering tool, i.e., the Gustafson-Kessel (GK) method [6]. On the other hand, the second step performs the identification of the controller structure and its parameters using the estimation method proposed by the same authors in [7]. This estimation approach can be considered as a generalization of the general least-squares method for hybrid models.

Under these assumptions, the TS fuzzy prototypes have the form of the model of Equation (14):

$$y_{k+1} = \frac{\sum_{i=1}^{M} \mu_i \left(\mathbf{x}_k\right) y_i}{\sum_{i=1}^{M} \mu_i \left(\mathbf{x}_k\right)} \tag{14}$$

where $y_i = \mathbf{a}_i^T \mathbf{x} + b_i$, with $\mathbf{a}_i$ the parameter vector (regressand), and b_i is the scalar offset. $\mathbf{x} = \mathbf{x}_k$ represents the regressor vector, which contain delayed samples of the signals u_k and y_k.

Note that the discrete-time description of Equation (14), after the proper estimation of the parameter vector [6], will be used for reconstructing the sampled outputs $P_g(t)$ and $\omega_g(t)$ of the continuous-time nonlinear model of Equation (9) fed by the sampled input signals $\beta(t)$ and $\tau_g(t)$.

The antecedent fuzzy sets μ_i that determine the switching among the different submodels i in Equation (14) are estimated using the input-output data acquired from the wind turbine simulator, i.e., the input and output sampled signals $\beta(t)$, $\tau_g(t)$ and $\omega_g(t)$ and $P_g(t)$. These data are organized into proper clusters where affine relations hold, as described in [6]. The consequent parameters $\mathbf{a}_i$ and b_i are also identified from these input-output data by means of the estimation methodology proposed in [7]. This identification scheme exploited for the estimation of the TS model parameters has been integrated into the FMID toolbox for MATLAB® by the authors. This approach is preferable when the TS model of Equation (14) is used as predictor, since it derives the consequent parameters via the so-called Frisch scheme, developed for the Errors-In-Variables (EIV) structures [7].

Once the description of the monitored process is obtained in the form of Equation (14), the data-driven approach for the design of the fuzzy controller proposed in this work is presented in Section 3.1.

The second approach exploited for obtaining the mathematical description of the wind turbine system under investigation is based on a recursive methodology, which will be used for the design of the second control strategy presented in Section 3.2. An on-line version of the batch Frisch scheme estimation methodology summarized above is recalled in the remainder of this section for estimating the parameters of dynamic EIV models. For the derivation of the adaptation law, an on-line bias-compensating algorithm is also implemented. Thus, the on-line Frisch scheme estimation is generalized to enhance its applicability to real-time implementations. Moreover, by means of an exponential forgetting factor included in the adaptation law, the algorithm is able to deal with Linear Parameter-Varying (LPV) structures, that are exploited in connection with the model-based design of the adaptive control scheme, presented in Section 3.2. Note that the adaptive algorithm proposed here exploits an iterative procedure that starts from an initial controller estimated off-line, for example using the baseline controller already implemented in the wind turbine simulator, and described in Section 2. This initial controller model is subsequently adapted on-line using the recursive laws in order to track the different operating conditions of the process under investigation.

Thus, the considered scheme is proposed for the on-line identification of the process modeled by the following transfer function $G(z)$:

$$G(z) = \frac{A(z^{-1})}{B(z^{-1})} = \frac{b_1 z^{-1} + \ldots + b_{n_b} z^{-n_b}}{1 + a_1 z^{-1} + \ldots + a_{n_a} z^{-n_a}} \tag{15}$$

where a_i, b_i, n_a and n_b represent the unknown parameters and the structure of the model, defining the polynomials $A(z^{-1})$ and $B(z^{-1})$, whilst z is the discrete-time complex variable.

The parameter vector describing the linear relationship is given by:

$$\theta = \left[a_1 \ \ldots \ a_{n_a} \ b_1 \ \ldots \ b_{n_b}\right]^T \tag{16}$$

whose extended version is defined as in Equation (17):

$$\bar{\theta} = \left[1 \ \theta^T\right]^T \tag{17}$$

An equivalent expression of the considered relations is obtained by using vector and matrix notations, in the form of Equation (18):

$$\psi_k^T \, \bar{\theta} = 0 \tag{18}$$

where the regressor vector ψ_k is defined as:

$$\psi_k = \left[-y_k \ -y_{k-1} \ \ldots \ -y_{k-n_a} \ u_{k-1} \ \ldots \ u_{k-n_b}\right]^T \tag{19}$$

where the subscript k denotes the sample index.

The Frisch scheme provides the estimates of the measurement errors affecting the input and output signals u_k and y_k, i.e., σ_u and σ_y and θ for a linear time-invariant dynamic system. Note that the polynomial orders n_a and n_b in the relation of Equation (15) are assumed to be fixed in advance.

From the Frisch scheme method, the following expression is considered:

$$\left(\Sigma_\psi - \Sigma_{\tilde{\psi}}\right) \bar{\theta} = 0 \tag{20}$$

where the noise covariance matrix is given by:

$$\Sigma_{\tilde{\psi}} = \begin{bmatrix} \sigma_y \, I_{n_a+1} & 0 \\ 0 & \sigma_u \, I_{n_b} \end{bmatrix} \tag{21}$$

which are approximated by the sample covariance matrix over N samples:

$$\Sigma_{\tilde{\psi}} \approx \frac{1}{N} \sum_{k=1}^{N} \psi_k \, \psi_k^T \tag{22}$$

Thus, the Frisch scheme aims at providing suitable noise variances σ_u and σ_y such that $\left(\Sigma_\psi - \Sigma_{\tilde{\psi}}\right)$ results to be a matrix singular positive semidefinite as it is rank-one deficient. On the other hand, the system represented by the expression of Equation (20) can be solved, and $\bar{\theta}$ represents its solution.

The expression of Equation (23) is determined:

$$\epsilon_k\left(\bar{\theta}\right) = A(z^{-1}) \, y_k - B(z^{-1}) \, u_k \tag{23}$$

whilst the so-called sample auto-covariance is defined in the form of Equation (24):

$$r_{\epsilon h, N} = \frac{1}{N} \sum_{l=1}^{N} \epsilon_l\left(\bar{\theta}\right) \, \epsilon_{l+h}\left(\bar{\theta}\right) \tag{24}$$

where the subscript h in Equation (24) indicates a time-shift.

The on-line control development requires a recursive estimate of the model parameters represented by the vector θ_k of Equation (15), while the input and output data u_k and y_k acquired on-line by the dynamic process of the wind turbine system. In fact, the adaptive control law computed

at time step k is based on the recursive estimate of a model of the process, which is derived exploiting the dynamic data up to the sample k. In this way, the algorithm of the Frisch scheme defined by the expressions of Equations (20), (22) and (24) is expressed by means of an on-line scheme.

Note that the expressions of Equations (22) and (24) are required in their recursive form. Therefore, whilst the derivation of the on-line form of the covariance matrix update is easily obtained as in the form of Equation (25):

$$\Sigma_{\tilde{\psi}_k} = \frac{k-1}{k}\,\Sigma_{\tilde{\psi}_k} + \frac{1}{k}\,\psi_k\,\psi_k^T \tag{25}$$

the formulation of the auto-covariance expression $r_{\epsilon h,k}$ can be obtained recursively for $1 \leq l \leq k$ only if the approximated expression of Equation (26) is considered:

$$\epsilon_l\left(\bar{\theta}_k\right) \approx \epsilon_l\left(\bar{\theta}_l\right) \tag{26}$$

for $l < k$. In this way, only the residual $\epsilon_k\left(\bar{\theta}_k\right)$ has to be computed at time step k using the lagged data in the vector ψ_k and the updated estimate $\bar{\theta}_k$ of the model parameters. The on-line computation of the expression of the auto-covariance matrix of Equation (27):

$$r_{\epsilon h,k} = \frac{k-1}{k}\,r_{\epsilon k,k-1} + \frac{1}{k}\,\epsilon_k\left(\bar{\theta}_k\right)\,\epsilon_{k+h}\left(\bar{\theta}_k\right) \tag{27}$$

can be achieved using only the vector $\epsilon_{k+h}\left(\bar{\theta}_k\right)$ at each time step. The initial values θ_0, $\Sigma_{\tilde{\psi}_0}$ and $r_{\epsilon 0,h}$ for the recursive algorithm are equal to the variables of the classic Frisch scheme batch procedure.

Since variations of system properties have to be tracked on-line, in order to cope with time-varying systems, this paper considers a further modification of the recursive estimation scheme. This point can be achieved by placing more emphasis on the more recent data, while forgetting the older ones. Therefore, the methodology represented by the expressions of Equations (25) and (27) with the approximation of Equation (26) is implemented by including the so-called exponential forgetting factor. This is achieved in practice by defining the new expressions of the sample covariance and auto-covariance matrices in the form of Equation (28):

$$\begin{cases} H_{\Sigma_{\tilde{\psi}_k}} &= \omega(\delta)\,\Sigma_{\tilde{\psi}_k} \\ h_{\epsilon h,k} &= \omega(\delta)\,r_{\epsilon h,k} \end{cases} \tag{28}$$

where $\omega(\delta)$ is a scaling factor that coincides with k when no adaptation is introduced. In this way, the updated expressions have the form:

$$\begin{cases} H_{\Sigma_{\tilde{\psi}_k}} &= (1-\delta)\,H_{\Sigma_{\tilde{\psi}_{k-1}}} + \delta\,\psi_k\,\psi_k^T \\ h_{\epsilon h,k} &= (1-\delta)\,h_{\epsilon h,k-1} + \delta\,\epsilon_k\left(\bar{\theta}_k\right)\,\epsilon_{k+h}\left(\bar{\theta}_k\right) \end{cases} \tag{29}$$

with $0 < \delta < 1$ representing the forgetting factor. Thus, the adaptive Frisch scheme algorithm is implemented via Equation (29) in three steps. First, θ_0, $\Sigma_{\tilde{\psi}_0}$ and $r_{\epsilon 0,h}$ with $h \leq n_a$ are initialized. Moreover, at each recursion step, by means of $r_{\epsilon h,k}$, the noise variances σ_u and σ_y are computed. Finally, at each recursion step, $\bar{\theta}_k$ is determined by solving Equation (20) via the expression of Equation (29). In this way, the vector θ_k contains the estimates of the model parameter derived at the step k.

The results achieved by the on-line identification method recalled in this section were obtained in the MATLAB® and Simulink® environments as summarized in Section 4.

Finally, once the parameters θ_k of the discrete-time linear time-varying model of the nonlinear dynamic process of Equation (9) have been computed at each time step k, the adaptive controller is derived as summarized in Section 3.2.

3.1. Data-Driven Fuzzy Control Strategy

This section describes the derivation of the fuzzy controller model. Once a reasonably accurate fuzzy description of the considered benchmark has been available, as described above, it is used off-line to directly estimate the nonlinear fuzzy controllers. As already remarked, this design procedure differs from the approach proposed in [29]. In fact, the control design proposed in this paper relies on the so-called inverse model principle, which is solved using the fuzzy identification approach recalled above.

Note that as explained in the following, the fuzzy methodology is exploited twice. First, the fuzzy modeling and identification approach is used to derive a fuzzy representation of the process under investigation, by means of its sampled inputs and outputs. Second, by means of this fuzzy model, and in particular using its state, the design of the fuzzy controller can be achieved. The derivation of the fuzzy controller model is performed by employing the states of the process fuzzy model. However, the estimation of the parameters of the fuzzy controller are achieved by minimizing the error between the reference power P_r and the controlled power $P_g(t)$, thus leading to maximize the wind turbine generated power.

With reference to stable fuzzy systems, whose inverted dynamics are also stable, a nonlinear controller can be simply designed by inverting the fuzzy model itself. Moreover, when modeling errors and disturbances are not present, this controller is able to allow for exact tracking with zero steady-state errors. However, modeling errors and disturbance effects are always present in real conditions, which can be tackled by directly identifying the controller model (i.e., the inverse controlled model) using the FMID approach. Differently from [29], a robust control strategy is thus achieved by minimizing a cost function which includes the difference between the desired and controller outputs, and a penalty on the system stability. In general, a nonconvex optimization problem has to be solved, which hampers the direct application of the proposed approach. However, the optimization scheme described in [7] can be exploited, which is based on a parametrized search technique applied at a higher level to formulate the control objectives and constraints.

Note that, as remarked in Section 2, the fuzzy approach proposed in this work is able to provide a high-fidelity description of the wind turbine behavior, which already includes uncertainty and disturbance, as described, e.g., in [22]. The fuzzy approach is thus used again to derive the formulation of the controller in the form of TS prototypes. The parameters of the controller fuzzy model are estimated by minimizing the difference between the monitored outputs and the reference ones, taking into account the disturbance and the uncertainty affecting the wind turbine process. Therefore, the approach proposed in this work is able to cope with external disturbance modeled in the wind turbine benchmark.

In this way, the estimated controller based on the process inverse model and approximated via a fuzzy prototype is able to describe the complete behavior of the monitored plant in its different working conditions (i.e., partial and full load situations). In fact, the rule-based fuzzy inference system of Equation (14) has been derived for modeling the wind turbine dynamic process of Equation (9) in its equivalent discrete-time form of Equation (30):

$$y_{k+1} = f\left(\mathbf{x}_k, u_k\right) \tag{30}$$

and, in particular, the TS fuzzy representation has the form of Equation (31):

$$y_{k+1} = \frac{\sum_{i=1}^{M} \mu_i^{(m)}\left(\mathbf{x}_k^{(m)}\right)\left(\mathbf{a}_i^{(m)}\,\mathbf{x}_k^{(m)} + b_i^{(m)}\right)}{\sum_{i=1}^{M} \mu_i^{(m)}\left(\mathbf{x}_k^{(m)}\right)} \tag{31}$$

The current state $\mathbf{x}_k = [y_k, \ldots, y_{k-n+1}, u_{k-1}, \ldots, u_{k-n+1}]^T$ and the input u_k represent the inputs that drive the model of Equation (31). Its output represents the prediction of the system output at

the next sample y_{k+1}. The model of Equation (31) requires the estimated membership functions $\mu_i^{(m)}$, the state $\mathbf{x}^{(m)}$ and the parameters $\mathbf{a}_i^{(m)}$, $b_i^{(m)}$ of the controlled system, which are denoted by the superscript (m).

Therefore, the input u_k generated by the control law feeds the monitored process such that its output y_{k+1} asymptotically follows the desired (reference) output r_{k+1}. This behavior is obtained by using the inverse model principle, represented by the expression of Equation (32):

$$u_{k+1} = f^{-1}\left(\mathbf{x}_k^c,\, r_k\right) \tag{32}$$

that is a nonlinear function of the vector $\mathbf{x}_k^c$ and the reference r_k.

However, in general, with reference to Equation (32), it is difficult to determine the analytical expression of the inverse function $f^{-1}(\cdot)$. Therefore, the methodology proposed in this work suggested to exploit the identified fuzzy TS prototype of Equation (31) to provide the particular state $\mathbf{x}_k^{(m)}$ at each time step k. In this way, from this mapping, the inverse mapping $u_{k+1} = f^{-1}\left(\mathbf{x}_k^{(c)},\, r_k\right)$ is directly identified the form of Equation (14), if the controlled system is stable, and in particular in the form of Equation (33):

$$u_{k+1} = \frac{\sum_{i=1}^{M} \mu_i^{(c)}\left(\mathbf{x}_k^{(c)}\right)\left(\mathbf{a}_i^{(c)}\,\mathbf{x}_k^{(c)} + b_i^{(c)}\right)}{\sum_{i=1}^{M} \mu_i^{(c)}\left(\mathbf{x}_k^{(c)}\right)} \tag{33}$$

where the state $\mathbf{x}_k^{(c)} = [\mathbf{x}_k^{(m)},\, r_{k-1},\, \ldots,\, r_{k-n+1}]^T$ and the reference r_k signal represent the inputs of the identified controller model. The model of Equation (33) contains the estimated membership functions $\mu_i^{(c)}$ and the parameters $\mathbf{a}_i^{(c)}$, $b_i^{(c)}$ of the identified controller model, that are denoted by the superscript (c). The complete scheme is outlined in Figure 5.

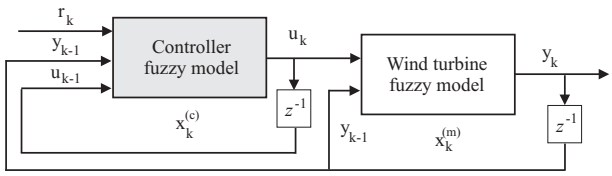

Figure 5. The fuzzy controller based on the inverse process model principle.

Note that Figure 5 sketches the general principle of the design of the controller for a system with input u_k and output y_k. On the other hand, the signal r_k represents the generic set-point to be tracked (i.e., P_r or ω_{nom}) depending on the working region (1 or 2) and the controlled output (i.e., the sampled signal $P_g(t)$ or $\omega_g(t)$). Under this assumption, the identification of the fuzzy controller parameters leads to minimize the difference between r_k and y_k. It is not required that r_k equals y_k, thus making the problem feasible within the selected degree of accuracy.

Figure 5 highlights the series connection between the controller models (i.e., the inverse process model identified using the fuzzy systems) and the process model itself (described by means of fuzzy models), which should lead to an identity mapping as in Equation (34):

$$y_{k+1} = f\left(\mathbf{x}_k^{(m)},\, u_k\right) = f\left(\mathbf{x}_k^{(m)},\, f^{-1}\left(\mathbf{x}_k^{(c)},\, r_k\right)\right) = r_{k+1} \tag{34}$$

where $r_{k+1} = f\left(\mathbf{x}_k^{(m)},\, u_k\right)$ for a proper value of u_k. However, the expression of Equation (34) holds in ideal conditions. However, the model-reality mismatch and measurement errors are properly managed by means of the fuzzy modeling scheme recalled in Section 3. In this way, the difference $|r_{k+1} - f\left(\mathbf{x}_k^{(m)},\, u_k\right)|$ can be made arbitrarily small by a suitable selection of the model parameters, i.e., the fuzzy membership functions $\mu_i^{(c)}$, the number of clusters M, and the regressand $\mathbf{a}_i^{(c)}$, $b_i^{(c)}$. Moreover, as highlighted in Figure 5, the fuzzy model of the process is used for providing the state

vector $\mathbf{x}_k^{(m)}$. Therefore, the state of the fuzzy controller $\mathbf{x}_k^{(c)}$ is updated using the process model state $\mathbf{x}_k^{(m)}$ and the reference input r_k. These computations are performed using standard matrix operations, thus making the algorithm suitable for real-time implementations [30].

Note that, with reference to the data-driven fuzzy approach, the stability issue is analyzed here both during the estimation stage and in simulation. On the one hand, the derivation of the fuzzy regulator is achieved in practice by means of a dynamic inversion of the process model of Equation (30). In fact, by using the fuzzy approach considered here, this dynamic inversion of the process model of Equation (31) is achieved by means of the computation of the TS fuzzy prototype describing the controller model of Equation (33). In more detail, the derivation of the fuzzy controller relies on two steps. In the first step, the fuzzy model of the controlled process of Equation (31) is obtained. This model is used to estimated the prototype of the fuzzy regulator of Equation (33). In fact, the fuzzy model of the process is exploited to generate the state $\mathbf{x}_k^{(m)}$ and the other signals y_k that are required for the identification of the fuzzy model of the controller. Note also that in this iterative procedure, the simulations are performed using only one-step-ahead predictions provided by the relations of Equations (31) and (33). In this way, the practical implementation of this algorithm does not suffer from convergence problems. Moreover, the minimization of the difference between the reference and the desired output $|r_{k+1} - f\left(\mathbf{x}_k^{(m)}, u_k\right)|$ with proper accuracy guarantees the derivation of the optimal fuzzy controller. The analytical proof of the stability of the overall system can rely on Lyapunov theory, as described, e.g., in [31]. On the other hand, the stability of the overall system is verified in simulation, when the proposed fuzzy regulator is applied to the wind turbine benchmark and the Monte Carlo tool is considered. These simulation results will be summarized in Section 4.

As already remarked, the effects of the model uncertainty and disturbance lead to a different behavior of the model with respect to controlled process, thus resulting in a mismatch between the process outputs y_k and their references r_k. This mismatch can be compensated by means of the on-line mechanism described by the expressions of Equations (31) and (33). These issues motivate the model-based strategy relying on the adaptive algorithm proposed in Section 3.2.

Note finally that the fuzzy controller proposed in this section and depicted in Figure 5 will replace the baseline wind turbine regulator of Section 2 and reported in Figure 4.

3.2. Model-Based Adaptive Control Scheme

This section describes the model-based adaptive control strategy used in connection with the on-line estimation scheme presented above. In more detail, with reference to the wind turbine system recalled in Section 2, adaptive controllers for processes of second order ($n_a = n = 2$) are designed. Moreover, the considered adaptive controllers are based on the trapezoidal method of discretisation.

With reference to Equation (15), the transfer function of the time-varying controlled system with $n_a = n_b = n = 2$ is considered, whose parameters estimated using the on-line identification approach recalled above:

$$\hat{\theta}_k = \left[\hat{a}_1,\, \hat{a}_2,\, \hat{b}_1,\, \hat{b}_2\right]^T \tag{35}$$

Note that the subscript k for model and controller parameters will be dropped in order to simplify equations and formulas.

The control law corresponding to the discrete-time adaptive controller in its difference form of Equation (36):

$$\begin{cases} \Delta e_k &= e_k - e_{k-1} \\ u_k &= \hat{K}_p \left[\Delta e_k + \frac{T_s}{\hat{T}_I} \frac{\Delta e_k}{2}\right] + u_{k-1} \end{cases} \tag{36}$$

with e_k representing the tracking error, with $e_k = r_k - y_k$, and r_k the reference (set-point) signal. T_s is sampling time. The controller parameters $\hat{K}_p$ and $\hat{T}_I$ are here time-varying and derived from the on-line

model parameters in the vector $\hat{\theta}_k$. The control law can be represented also in its feedback formulation as described by Equation (37):

$$u_k = \hat{q}_0\, e_k + \hat{q}_1\, e_{k-1} + u_{k-1} \tag{37}$$

where the new controller variables $\hat{q}_0$ and $\hat{q}_1$ (or $\hat{K}_p$ and $\hat{T}_I$) are derived from the relations of Equation (38):

$$\begin{cases} \hat{q}_0 &= \hat{K}_p \left(1 + \frac{T_s}{2\,\hat{T}_I}\right) \\ \hat{q}_1 &= -\hat{K}_p \left(1 - \frac{T_s}{2\,\hat{T}_I}\right) \end{cases} \tag{38}$$

where the parameters $\hat{K}_p$ and $\hat{T}_I$ are functions of the (time-varying) critical gain and the critical period of oscillations, respectively, K_{P_u} and T_u:

$$\hat{K}_p = 0.6\,\hat{K}_{P_u},\ \hat{T}_I = 0.5\,\hat{T}_u \tag{39}$$

that depend on the time-varying model parameters in the vector $\hat{\theta}_k$. In particular, when considering a second order model described by its (time-varying) parameters $\hat{a}_2$, $\hat{a}_1$, $\hat{b}_2$ and $\hat{b}_1$, the variables $\hat{K}_{P_u}$ and $\hat{T}_u$ required by the Ziegler-Nichols method used in this work are computed at each time step k from the following relations [32,33]:

$$\begin{cases} \hat{K}_{P_u} = \frac{\hat{a}_1 - \hat{a}_2 - 1}{\hat{b}_2 - \hat{b}_1} \\ \hat{T}_u = \frac{2\pi T_s}{\arccos \hat{\gamma}}, \quad \text{with } \hat{\gamma} = \frac{\hat{a}_2\,\hat{b}_1 - \hat{a}_1\,\hat{b}_2}{2\,\hat{b}_2} \end{cases} \tag{40}$$

In this way, the adaptive discrete-time linear controllers of Equations (36) or (37) are designed on the basis of the time-varying linear model of Equation (15) estimated via the on-line identification scheme from the data of the nonlinear wind turbine process of Equation (9).

Note that the adaptive regulators considered in this section were implemented in the Simulink® environment, integrating also the on-line estimation scheme recalled above.

The simulation set-up employs three adaptive regulators used for the control of the blade pitch angle $\beta(t)$, and the generator control torque $\tau_r(t)$, in the partial and full load working conditions, by using the controlled outputs $\omega_g(t)$ and $P_g(t)$. The complete block scheme is shown in Figure 6.

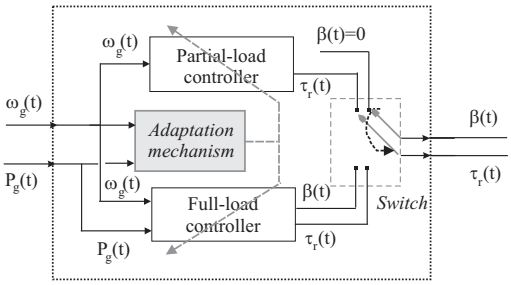

Figure 6. Diagram of the adaptive control strategy.

Note that, the adaptive control scheme represented in Figure 6 will replace the baseline wind turbine controller recalled in Section 2 and depicted in Figure 4. In this way, the adaptive controller should be able to manage possible uncertainty affecting the wind turbine system, thus allowing one to improve the performance of the baseline wind turbine control described in Section 2.

Note that an important point concerns the stability issue when the switching of the controllers is considered, and it can be solved as bumpless transfer for adaptive control. In more detail, in the adaptive control setting, the controller output can have undesired transients (bumps), if a current on-line controller and a new controller to be switched have different outputs at the switching instant. To attenuate these bumps associated with controller switching, which could lead to stability problems,

a variety of bumpless transfer methods have been suggested. As in this case, the plant is not precisely known at the outset, and the goal of adaptive control is to change the controllers to improve performance as plant data begins to reveal some information about the plant. Thus, in adaptive switching control an exact plant is generally unavailable at the time of switching. Moreover, in the adaptive application considered in this work where the true plant model may only be poorly known at controller switching times, it may be preferable to employ a bumpless transfer technique that does not depend on a precise knowledge of the true plant model. Therefore, the bumpless transfer method presented in [34,35] based on the slow decomposition of the controller is considered. It consists of a method that can be implemented without precise knowledge of the true plant at switching times. In particular, by appropriately re-initializing the states of the controller modes at switching times, this method ensures that not only will the controller output be continuous, but also that it avoid fast transient bumps after switching.

Another key aspect concerns the possible non-minimum phase behavior of the considered wind turbine. In this case, the self-tuning design procedure represented by Equations (39) and (40) would lead to poor performances. However, it is worth noting that according to Section 2, there are two possible regions of turbine operation, namely the high and low wind speed regions. High-speed operation is frequently bounded by the speed limit of the machine. Conversely, regulation in the low-speed region is usually not restricted by speed constraints. However, the system has possible non-minimum phase dynamics in this low-speed region. Moreover, this behavior in the low-speed region can be observed for very low tip-speed-ratio, i.e., when λ is near to zero. However, as presented by the paper in Section 4, the condition $\lambda \approx 0$ is always not satisfied, also for low wind speed. Therefore, the benchmark under consideration can present non-minimum features only for working conditions different from the ones considered in Section 2. However, alternative design methodologies that take into account time delay behavior can be found, e.g., in [36]. Considering again Equation (46), the Taylor approximation of a time delay transfer function leads to verify that an inverse response time constant T_o^{inv} (negative numerator time constant in Equation (46)) may be approximated as a time delay:

$$(-T_o^{inv}\, w + 1) \approx e^{-T_o^{inv}\, w} \tag{41}$$

This represents the deteriorating effect of an inverse response similar to that of a time delay. In the same way, a lag time constant τ_s may be approximated again as a time delay:

$$\frac{1}{\tau_s\, w + 1} \approx e^{-\tau_s\, w} \tag{42}$$

Furthermore, considering the product of Equations (41) and (42), it follows that the effective delay L of Equation (43) can be taken as the sum of the contribution from the various approximated terms T_o^{inv} and τ_s. In addition, for digital implementation with sampling period T_s, L can consider also the contribution of the D/A converter $T_s/2$. Therefore, the approximation of Equation (43) is valid, and an approximate first-order time delay stable model is obtained as already shown by Equation (43):

$$\frac{k}{w\, \tau_o + 1} \approx e^{-w\, L} \tag{43}$$

where k is the model gain, τ_o the dominant lag time constant, and L the effective time delay. Under these assumptions, the following rules for the tuning of the PI controller can be exploited for first-order time delay (non-minimum phase) models:

$$\begin{cases} \hat{K}_p &= \frac{1}{k}\, \frac{\tau_o}{\tau_c + L} \\ \hat{T}_I &= \min\{\tau_o\, , 4\, (\tau_c + L)\} \end{cases} \tag{44}$$

where τ_c is the desired first-order closed-loop response time and represents the only tuning parameter. Small values of τ_c lead to response fast speed, whilst large values for stable and robust behavior. A good rule would suggest to set $\tau_c = L$ for fast response with good robustness properties [36].

It is worth noting that the work [37] provided an analytical demonstration of the stability of an adaptive control scheme for wind turbines.

Finally, Section 4 will show the achieved results regarding the design and the application of the adaptive controller to the data from the wind turbine benchmark.

4. Simulations and Comparisons

This section presents the simulation results achieved with the proposed control methods relying on both the fuzzy modeling technique oriented to the identification of the fuzzy controller description, and the adaptive control strategy using the on-line estimated models. The simulations obtained with these regulators are summarized in Section 4.1. Moreover, the reliability and robustness analysis, followed by extended comparisons with respect to different control solutions are reported in Sections 4.2 and 4.3, respectively. Further simulations will be reported in Section 4.4 for verifying the stability properties of the proposed solutions, whilst Section 4.5 will provide some final remarks.

4.1. Controller Performance Tests

Regarding the fuzzy modeling and identification method, the GK clustering algorithm recalled in Section 3 with a number $M = 3$ of clusters and delays $n = 2$. These variables were applied for clustering the first data set consisting of $\{P_{g_k}, \omega_{g_k}, \beta_{r_k}\}$. A number of samples $k = 1, 2, \ldots, N$ were considered with $N = 440 \times 10^3$. The same number of clusters and shifts were exploited for clustering the second data set $\{P_{g_k}, \omega_{g_k}, \tau_{g_k}\}$. After this procedure, the structures of the TS prototypes were derived for each output y_k equal to P_{g_k} and ω_{g_k}. In this way, the two continuous-time outputs $y(t) = [\omega_g(t), \tau_g(t)]$ of the wind turbine continuous-time model of Equation (9) are approximated by two TS fuzzy prototypes of Equation (14).

The performances of the fuzzy models that are derived using the procedure described above can be evaluated using the so-called Variance Accounted For (VAF) parameter [6]. In particular, the TS fuzzy model reconstructing the first output has a VAF index bigger than 90%, whilst for the second one, it was higher than 99%. This means that the fuzzy prototypes are able to describe the behavior of the controlled process with very good precision. These estimated TS fuzzy models have been used for the derivation of the fuzzy controllers and applied to the considered wind turbine benchmark.

Two fuzzy controllers with 2 inputs and 1 output have been used for the control of the wind turbine system. As shown in Figure 4, these controllers are both fed by the sampled signals P_{g_k}, ω_{g_k} (i.e., the outputs of the wind turbine system) for the generation of the sampled signals β_k and $\tau_r(t)$ (i.e., the control inputs for the wind turbine system). By using the inverse model principle, they were estimated exploiting the methodology recalled in Section 3.1. Again, the GK fuzzy clustering method has lead to two fuzzy regulators applied to the data sets $\{\beta_k, P_{g_k}, \omega_{g_k}\}$ and $\{\tau_{g_k}, P_{g_k}, \omega_{g_k}\}$, respectively, with $M = 3$ clusters and $n = 3$ lagged signals.

The controller performances were verified and validated via extensive simulations by considering different data sequences generated via the wind turbine simulator. Table 4 reports the values of the delay time T_d, settling time T_a, maximum overshoot $S\%$ and the per-cent Normalized Sum of Squared tracking Error ($NSSE\%$) index defined in Equation (45):

$$NSSE\% = 100 \sqrt{\frac{\sum_{k=1}^{N} \left(r_k - y_k\right)^2}{\sum_{k=1}^{N} r_k^2}} \tag{45}$$

Note that in partial load operation (Region 1), the performance is represented by the comparison between the power produced by the generator, $y_k = P_{g_k}$, with respect to the theoretical maximum

power output, $r_k = P_r$. On the other hand, in full load operation (Region 2), the tracking error is given by the difference between the generator speed, $y_k = \omega_{g_k}$ and its nominal value, $r_k = \omega_{nom}$. The achieved results are shown in Figure 7 for the case of the identified fuzzy controllers.

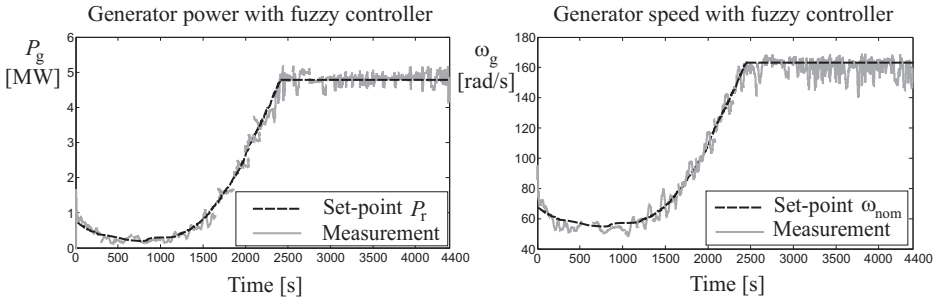

Figure 7. Generator speed ω_g and power P_g (bold gray line) with respect to their references (dashed black line) ω_{nom} and P_r with the fuzzy controllers.

Figure 7 depicts the signal representing the controlled generator speed ω_g and the generated power P_g in gray bold gray line with respect to their desired values ω_{nom} and P_r in dashed black line, respectively. It can be noted that in both partial and full load conditions, the fuzzy controllers are able to track the reference signals, as recalled in Section 2. Note that the performance of the fuzzy regulators are better than those achieved via the baseline governors, which were tuned with frequency approaches described in [23,24].

With reference to the second adaptive design approach using adaptive solutions, the two outputs $P_g(t)$ and $\omega_g(t)$ of the wind turbine continuous-time nonlinear model of Equation (9) were approximated by two second-order time-varying discrete-time models of Equation (15) with two inputs and one output. Using these two LPV prototypes, the model-based approach for determining the adaptive controllers recalled in Section 3.2 was exploited and applied to the wind turbine benchmark of Section 2. Thus, according to Section 3.2, the parameters of the adaptive controllers were computed on-line. In particular, for each output, two second-order ($n_a = n_b = 2$) time-varying prototypes were identified, and the adaptive regulator parameters in Equations (36) or (37) were computed analytically at each time step k. Also in this case, with reference to the adaptive controller structure of Equations (36) or (37), the parameters of the adaptive controllers were tuned on-line via the Ziegler-Nichols rules, applied to the LPV models. This adaptive procedure is already implemented and available in [32,33]. In this way, if both the model on-line parametric identification and the regulator recursive tuning procedure are exploited, the parameter adaptation mechanisms should lead to good control performances.

The simulations with the adaptive regulators have been obtained in the same situation of the fuzzy controllers. In this case, three on-line regulators were exploited for the compensation of both the blade pitch angle $\beta(t)$ and the generator torque $\tau_g(t)$, in Region 1 and Region 2. The adaptive algorithm described above run with initial values for its parameters reported in Table 3.

Table 3. Initialization parameters of the adaptive algorithm.

Recursive Algorithm Parameter	Value
$\bar{\theta}(0)$	$[0.1,\ 0.15,\ 0.20,\ 0.25\,0.30,\ 0.35]^T$
$\Sigma_{\tilde{\psi}}(0)$	$10^{-1}\ I_7$
δ	0.995

Also with reference to the model-based adaptive approach, Figure 8 depicts both the controlled outputs P_g and ω_g in bold gray lines with respect to their reference values P_r and ω_{nom}, respectively,

in dashed black lines. As will be seen in the following, also for the case of the adaptive regulators, Figure 8 highlights that this approach leads to interesting performances.

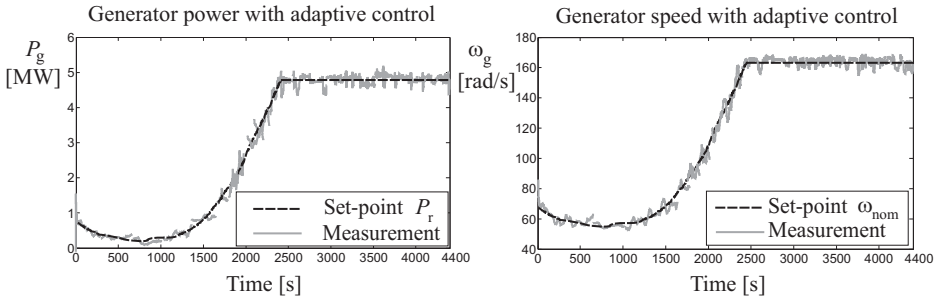

Figure 8. P_g and ω_g tracking capabilities in partial and full load conditions with the adaptive controllers.

Note that the recursive scheme is able to react actively with respect to variations of the working conditions of the wind turbine system. In fact, the fuzzy method can be considered a passive (even if robust) control solution, since the controllers are identified to passively tolerate the disturbance acting on the system. On the other hand, the adaptive methodology is able to counteract any variation or disturbance effects of the controlled process, thus representing an active control solution. These definitions were provided for different frameworks, e.g., in [38,39].

As further example, Figure 9 depicts the main wind turbine model variables in full load working conditions.

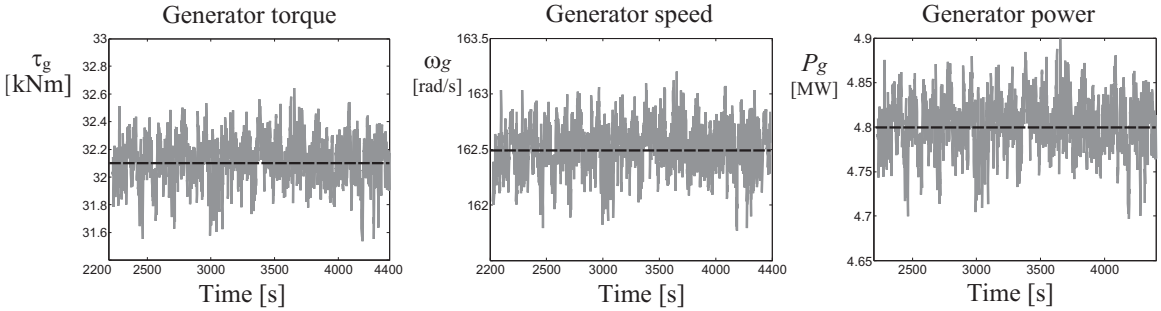

Figure 9. Variables of the benchmark in full load operation.

In particular, Figure 9 depicts the wind signal $v(t)$, the generator speed ω_g and power P_g, and the control input β.

In order to analyze the performance of the proposed adaptive strategy, Table 4 reports also the T_d, T_a, $S\%$ and $NSSE$ values computed for these controllers.

Table 4. Controllers in partial and load operations: T_d, T_a, $S\%$ and $NSSE\%$ values.

Controller Type	Partial Load NSSE%	Full Load NSSE%	Delay Time T_d	Settling Time T_a	Max. Overshoot S%
Baseline governors	46.68%	20.96%	0.89 s	2 s	21%
Fuzzy controllers	37.17%	17.85%	0.02 s	0.26 s	7%
Adaptive controllers	28.73%	13.67%	0.01 s	0.14 s	3%

According to the simulation results summarized in Table 4, good tracking capabilities of the suggested adaptive controllers seem to be reached, and they are better than both the fuzzy regulators and the baseline governor, recalled in Section 2.

4.2. Robustness Analysis

This section summarizes further simulation results that concern the evaluation of the achieved characteristics of the developed control strategies when the effects of uncertainty and disturbance are taken into account.

In particular, the wind turbine benchmark in the MATLAB® and Simulink® environments can vary the variables and the parameters of the simulated process in a statistical way. In this way, it is possible to analyze the effects of the model-reality mismatch and the measurement errors on the designed controllers. Moreover, a Monte Carlo analysis is also considered since it represents a practical approach for validating and verifying the features of the developed control schemes when applied to the considered wind turbine process. The same approach was for suggested for the first time by the same authors in [40] and applied to a different simulated system. The Monte Carlo tool is very useful in this case since the behavior of control strategies designed assuming the nominal plant depends on both the model-reality mismatch and the measurement errors.

Under these considerations, the uncertainty values of the parameters and variables of the wind turbine simulator considered in this work are summarized in Table 5. Therefore, the Monte Carlo analysis was achieved by modeling these parameters and variables as Gaussian stochastic processes, with mean values equal to the nominal ones, and standard deviations corresponding to realistic error values, typical of wind turbine models [3].

Table 5. Wind turbine uncertain variables.

Model Variable/Parameter	Standard Deviation
$\beta(t)$	11%
$\omega_g(t)$	18%
$\tau_g(t)$	21%
$P_g(t)$	20%
Pitch 2nd order model natural frequency and damping ratio	49%
Drive train model efficiency	5%
Converter 1st order model time constant	50%

Therefore, for the evaluation of the reliability and robustness characteristics of the designed control schemes, the average values of the $NSSE\%$ index were computed and evaluated in simulation via 1000 Monte Carlo runs. Note that, as already remarked in Section 3, proper algorithms were exploited for guaranteeing the derivation of controller models that lead to stable closed loops. On the other hand, the stability of the closed loop system when adaptive algorithms are exploited was investigated in [37].

Note however that, if unstable models should be obtained due to large uncertainties of Table 5, gain and phase margin requirements have to be included in the controller design, as described, e.g., in [41], and the controller parameters can be computed using the w-plane design. In this case, it can be shown that the model of Equation (15) with $n_a = n_b = n = 2$ is transformed into its equivalent description of Equation (46):

$$\frac{T_s\,(b_1\,T_s - b_2\,T_s)\,w^2 + (-2\,b_1\,T_s + 2\,b_2\,T_s + T_s\,(2\,b_1 + 2\,b_2))\;w - 4\,b_1 - 4\,b_2}{(a_1\,T_s^2 - T_s^2 - a_2\,T_s^2)\,w^2 + (4\,a_2\,T_s - 4\,T_s)\,w - 4 - 4\,a_2 - 4\,a_1} \approx \frac{k}{w\,\tau_o - 1}\,e^{-w\,L} \tag{46}$$

Under the validity of the approximation of Equation (46), which neglects the fast dynamic stable modes, and consider only the unstable pole τ_o with the effective delay L (see, e.g., the approximation in [36]), the adaptive controller parameters are computed via the relations of Equation (47):

$$\begin{cases} K_p &= \dfrac{\delta\,\tau_o}{A_m\,k} \\ T_I &= \dfrac{1}{\frac{\pi}{2}\,\delta - \delta^2\,L - \frac{1}{\tau_o}} \\ \delta &= \dfrac{A_m\,\phi_m + \frac{\pi}{2}\,A_m\,(A_m - 1)}{(A_m^2 - 1)\,L} \end{cases} \tag{47}$$

The relations of Equation (47) provide the parameters K_p and T_I of the adaptive regulator that allow one to obtain the gain and phase margins (A_m, ϕ_m) for the identified (unstable) model of Equation (46). Note that, even if approximations are used to derive the tuning formulas of (47), it can be seen that the achievable gain and phase margins can be quite close to the specified ones, and in general within a 5% of maximal error.

After these considerations, Table 6 reports the average T_d, T_a, $S\%$ and $NSSE\%$ values by considering the effects on the input and output measurements given by the alteration of the model variables and parameters reported in Table 5. Moreover, Table 6 shows how the considered control strategies, and especially the adaptive approach, is able to achieve excellent performances even in the presence of considerable error and uncertainty effects.

Table 6. Monte Carlo analysis for the considered control schemes.

Control Strategy	Partial Load NSSE%	Full Load NSSE%	Delay Time T_d	Settling Time T_a	Max. Overshoot S%
Baseline governors	48.23%	21.75%	0.91 s	2.5 s	23%
Fuzzy controllers	37.19%	17.94%	0.04 s	0.34 s	8%
Adaptive controllers	24.52%	13.72%	0.02 s	0.18 s	4%

The achieved results highlight also that Monte Carlo tool represents an effective and practical instrument for validating and verifying in simulation the design reliability and robustness of the considered control methodologies with respect to modeling uncertainty and measurement errors.

Note finally that the results summarized in Table 6 serve to verify and validate the overall behavior of the developed control techniques, when applied to the considered wind turbine benchmark. In more detail, the values of the $NSSE\%$ index highlights that when the mathematical description of the controlled dynamic processes can be included in the control design phase, model-based techniques yield to the best performances, even if an optimization procedure is required. However, when modeling errors are present, the off-line learning exploited by the fuzzy regulators allows one to achieve results better than classical schemes. For example, this consideration is valid for the baseline PID controllers recalled in Section 2 derived via trial and error procedures. On the other hand, fuzzy controllers have led to interesting tracking capabilities. With reference to the adaptive scheme, it takes advantage of its recursive features, since it is able to track possible variations of the controlled systems, due to operation or model changes. However, it requires quite complicated and not straightforward design procedures relying on adaptive and recursive algorithms. Therefore, fuzzy-based schemes use the learning accumulated from off-line simulations, but the training stage can be computationally heavy. Finally, concerning the standard PID control strategy, it is rather simple and straightforward, even if the achievable performances are quite limited when applied to nonlinear dynamic processes.

4.3. Performance Verification and Comparisons

The evaluation of the performances of the data-driven and model-based control strategies considered in this paper has been evaluated also on the basis of the following performance metrics, borrowed and modified from the fault diagnosis framework [40]:

- False Tracking Rate (FTR): the ratio between the total number of wrongly reference tracking and the number of simulations;

- Missed Tracking Rate (MTR): the ratio between the total number of missed reference tracking and the number of simulations;
- Correct Tracking Rate (CTR): the ratio between the number of correct reference tracking and the number of simulations;
- Mean Tracking Delay (MTD): the delay time between the reference tracking and the reference timing.

With reference to the indices above, note that the CTR index is complementary to MTR, since they refer to the tracking capabilities in the presence of uncertainty and disturbance. In contrast, the FTR index describes the tracking performance achieved only by the control designs, without considering any errors or anomalies occurring in the system. On the other hand, the MTD index considers the average delay occurring during the tracking of the reference signals.

Also in this case, a proper Monte Carlo analysis has been performed in order to compute these performance metrics and to test the robustness of the considered control schemes. A set of 1000 Monte Carlo runs has been performed, during which realistic wind turbine uncertainties have been considered as described in Table 5. Moreover, in addition to the considered fuzzy and adaptive strategies, the performance metrics of other control schemes are analyzed.

The first alternative approach considered here uses a Support Vector machine based on a Gaussian Kernel (GKSV) originally developed in [42] and it was exploited here for control purpose. The scheme defines a vector of features for each working condition of the wind turbine, which contains relevant signals obtained directly from measurements, filtered measurements or their combinations. These vectors are subsequently projected onto the kernel of the Support Vector Machine (SVM), which provides suitable control sequences for all of the defined working conditions.

The second scheme consists in an Estimation-Based (EB) solution shown in [43]. In particular, a bank of observers is designed to estimate the control signals that have to feed the controlled process. These observers were designed on the basis of a system linear model.

The third method relying on Up-Down Counters (UDC) was addressed in [44]. These tools, are commonly used in the aerospace framework, and they provide a different approach to the decision logic usually applied to the control. Indeed, the design of the control signals involves discrete-time dynamics and is not simply a function of the plant working conditions.

The fourth approach refers to Combined Observer and Kalman (COK) filter methods [45]. It relies on an observer used as a control signal residual generator, when the wind speed is considered a disturbance. This observer was designed to decouple the disturbance and simultaneously achieve optimal reference tracking in a statistical sense.

Finally, the fifth method is a General Fault Model (GFM) scheme, which is a method of automatic design [46]. The design strategy consists of three main steps. In the first step, a large set of potential controllers is designed. In the second step, the most suitable control signals to be included in the final system are selected. The third step tests the selected set of control laws, on the basis of extended comparisons of the estimated probability distributions of the tracking errors, evaluated with and without uncertainty or disturbance effects.

The results of the comparative analysis are summarized in Table 7, tacking into account the uncertainty effects reported in Table 5. The different control approaches are analyzed and compared.

The results summarized in Table 7 serve to highlight the efficacy of the considered control solutions also with respect to different schemes. In details, both the data-driven and model-based approaches seem to work better than other approaches, and they have a noteworthy performance level considering the mean delay time, which is significantly low. Furthermore, the FTR and the MTR indices are lower than those of other approaches. However, for both model-based and data-driven designs, optimization stages are required, for example for the selection of the GK clustering algorithm. Furthermore, the GKSV approach presents quite high delays, with big FTR and MTR. EB has comparable performance with respect to GKSV in terms of FTR, CTR and MTR, but with lower MTD. UDC can show quite high FTR in both the working conditions. COK and GFM have similar

performances, with important MTD, FTR and MTR. However, in general, the proposed data-driven and model-based approaches are able to achieve good tracking capabilities, with minimum MTD, and higher CTR with respect to the other control methodologies.

Table 7. Comparison of the different control strategies applied to the wind turbine benchmark. GKSV, Support Vector machine based on a Gaussian Kernel; EB, Estimation-Based; UDC, Up-Down Counters; COK, Combined Observer and Kalman; GFM, General Fault Model; FTR, False Tracking Rate; MTR, Missed Tracking Rate; CTR, Correct Tracking Rate; MTD, Mean Tracking Delay.

Working Condition	Index	GKSV	EB	UDC	COK	GFM	Fuzzy	Adaptive	Baseline
Partial Load	FTR	0.234	0.224	0.123	0.003	0.235	0.001	0.018	0.403
	MTR	0.343	0.333	0.232	0.029	0.532	0.003	0.001	0.596
	CTR	0.657	0.667	0.768	0.971	0.468	0.997	0.999	0.404
	MTD (s)	47.24	44.65	69.03	19.32	13.74	0.08	0.08	70.87
Full Load	FTR	0.001	0.001	0.001	0.001	0.001	0.001	0.001	0.003
	MTR	0.002	0.003	0.002	0.003	0.002	0.001	0.001	0.003
	CTR	0.978	0.977	0.987	0.977	0.982	0.999	0.999	0.865
	MTD (s)	0.03	0.03	0.04	0.32	0.05	0.02	0.01	0.89

4.4. Stability Analysis

The stability properties of the proposed control strategies have been checked by means of a Monte Carlo campaign based on the wind turbine benchmark. In fact, the Monte Carlo analysis represents the only method for estimating the efficacy of the developed control schemes when applied to the monitored process. It is worth noting that the works [31,37] suggested an analytical demonstration of the stability of fuzzy and adaptive control schemes, whilst some practical issues were remarked in Sections 3.1 and 3.2 for the fuzzy approach and the adaptive strategy, respectively.

All simulations were performed by considering noise signals modeled as Gaussian processes, according to the standard deviations reported in Table 5. Different wind sequences were generated by the wind turbine benchmark simulator. Moreover, the initial conditions of the dynamic models recalled in Section 2 (i.e., the drive-train, the generator/converter, and the pitch system) were changed randomly. Therefore, the random wind signal $v(t)$, the parameters of Table 5, and the dynamic model initial conditions allowed obtaining different sequences of the wind turbine signals $\beta(t)$, $\tau_g(t)$, $\lambda(t)$, $\omega_g(t)$, and $P_g(t)$ for each Monte Carlo simulation.

As an example of a single Monte Carlo run, Figure 10 highlights that the main wind turbine model variables, such as the generator torque $\tau_g(t)$, the tip-speed-ratio $\lambda(t)$, and the generator power $P_g(t)$ remain bounded around the reference values, proving the overall system stability in simulation, even in the presence of disturbance and uncertainty. These results refer to the case of full load operation with the data-driven fuzzy controllers.

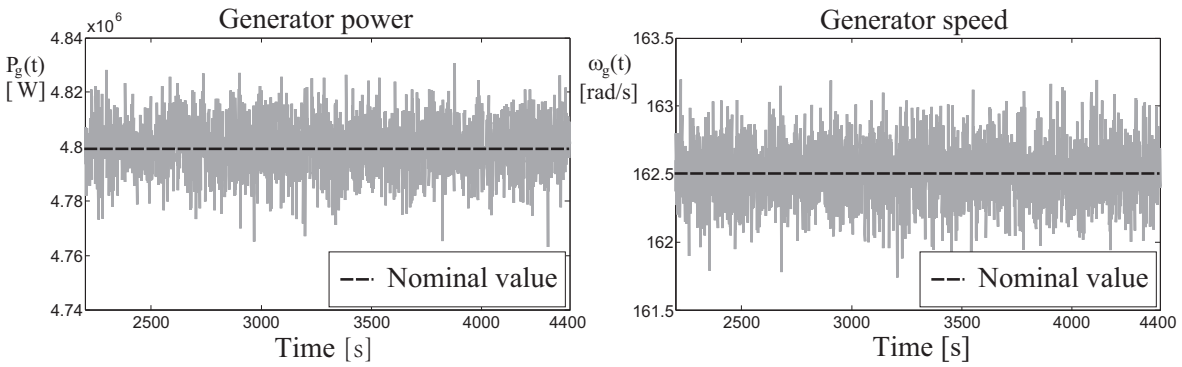

Figure 10. Sensitivity analysis in full load conditions with the data-driven fuzzy regulators.

As further Monte Carlo example run, the results achieved with the model-based adaptive controller in full load are summarized in Figure 11.

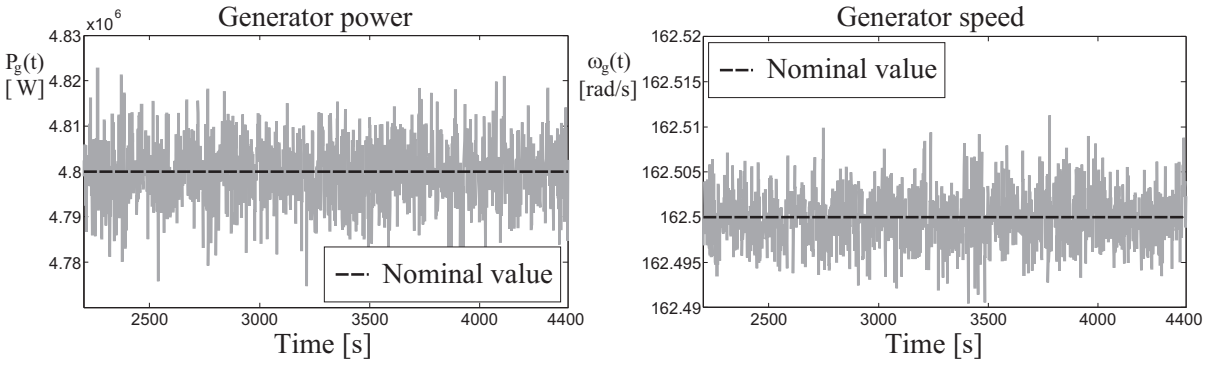

Figure 11. Simulations in full load with the adaptive controllers.

Figure 11 depicts the perturbed signals representing the generator speed $\omega_g(t)$ and power $P_g(t)$, with respect to their nominal values. Also in this case, the main wind turbine variables remain bounded around the reference values, thus assessing the overall system stability in simulation, even in the presence of modeling errors and disturbance.

4.5. Final Remarks

The application examples considered in this paper have highlighted how the availability of an accurate simulator of a wind turbine system has reached its maturity level, as shown in Section 2. Therefore, most of the insight has been given into the control techniques, resulting in advanced and refined solutions, which can include a variety of sub-functions, such as the optimal set-point generation, the set-point following and supervisory tasks, when considering the different operation requirements. In addition to these aspects, advanced control strategies relying on two approaches, such as data-driven and model-base strategies, have been considered for comparison purposes, as articulated in Section 3.

It is clear that further 'levels' of control can be required in wind turbine applications, which were not considered in this study. There is a top level of supervisory control that verifies the available energy source and can limit the operation of the device accordingly, also in case of extreme conditions. These limitations may be implemented in order to preserve the system integrity, ensure safe operation or be required by legislation, as for the case of wind turbines and their cut-out wind speed limits. This situation is represented in Figure 3b, when the wind turbine operates in full load conditions (above the rated wind speed). On the other hand, it is also developed to work for generating electric energy when the wind speed is below its rated wind speed and an optimal reference has to be tracked, as highlighted by Equation (10). In this case, the maximum-energy transfer is required. However, wind turbine plants can also work outside their nominal operating conditions, and some supervisory module may be required to ensure the device integrity. This supervisory strategy is important, and it can represent the key point also for the safety of these energy conversion systems, as discussed by the authors, e.g., in [47], but not considered here.

Control systems remain often hidden, since they are incorporated within the devices themselves. They are fundamental for energy conversion systems and can represent the key point technologies for achieving optimal performance, improving energy conversion and guaranteeing safety. Moreover, the solution of incorporating control technology is very appealing for several systems, since the addition of extra control features may be obtained by simply adding software functions [48]. In some cases, this solution avoids the requirement of expensive additional sensors and actuators [49]. However, this relatively straightforward implementation can require both sophisticated control methodologies and complicated mathematical formulations. For example, concerning wind turbines,

many high-performance model-based control schemes can require high-fidelity simulators of the controlled plants [50]. Nevertheless, there is usually a trade-off between the incorporation of advanced control techniques and the requirement of expensive technology, both used to improve the performance, reliability and safety of the monitored systems.

In particular with reference to the proposed strategies, some further comments can be drawn in general, concerning the key aspects of these advanced control solutions, with respect to the baseline PID governors proposed in Section 2. The $NSSE\%$ values obtained with the proposed control strategies are lower. Standard industrial controllers, such the classic PID regulators recalled in Section 2, are quite simple and have the benefit of quite straightforward tuning of their parameters. However, when exploited for controlling nonlinear dynamic processes, the control laws may lead to limited performances. Therefore, this point motivates the use of more advanced control solutions, as highlighted by the results summarized in this section. In particular, when the modeling of the dynamic process can be perfectly achieved, model-based control strategies generally represent the best option. However, when modeling errors and uncertainty effects are important, control schemes relying on active or adaptation mechanisms can show interesting features. On the other hand, with reference to pure data-driven methodologies, and in particular to the design of the fuzzy controllers, the off-line optimization can allow one to reach quite good results. Other control techniques can take advantage of their robustness characteristics, but with quite complicated and not direct design methodologies. Therefore, concerning the considered methods relying on adaptive and fuzzy tools, they can appear rather straightforward, even if optimization strategies have to be applied.

Finally, in theory, the development of the design of a complete plant should be performed from the top down. However, physical systems are often designed by discipline-specific experts, whilst the related control aspects are considered in a further stage by control engineers. Such an approach, even if common in industrial applications of control, is non-optimal, and integrated approaches should be considered, as described, e.g., in [51].

5. Conclusions

The work addressed two control examples for a wind turbine dynamic simulator, since it was proposed as a benchmark representing a complex dynamic system driven by stochastic disturbances and uncertain load conditions. Moreover, the aerodynamic models of these processes are nonlinear, thus making their modeling a challenging problem. Therefore, the design of control strategies for these complex processes has to consider these aspects. In this way, the paper analyzed the design of two data-driven and model-based control methodologies, which represented viable, reliable and robust control schemes for the proposed wind turbine benchmark. Experiments with the wind turbine simulator and the Monte Carlo tool were the practical instruments for assessing the most important characteristics of the developed control methodologies, when the model-reality mismatch and measurement errors were also considered. The analyzed control methods were finally compared with respect to different control solutions proposed in the related literature, in order to highlight advantages and drawbacks of the developed strategies. The obtained results showed that the considered solutions represent viable, robust and reliable control applications to real wind turbine systems.

Acknowledgments: The research work has been supported by the FAR2017local fund from the University of Ferrara. On the other hand, the costs to publish in open access have been covered by the FIR2018local fund from the University of Ferrara.

Author Contributions: Silvio Simani conceived of and designed the simulations; moreover, he analyzed the methodologies and the achieved results and, together with Paolo Castaldi, wrote the paper.

Conflicts of Interest: The authors declare no conflicts of interest.

References

1. Johnson, K.E.; Pao, L.Y.; Balas, M.J.; Fingersh, L.J. Control of variable-speed wind turbines: Standard and adaptive techniques for maximizing energy capture. *IEEE Control Syst. Mag.* **2006**, *26*, 70–81, doi:10.1109/MCS.2006.1636311.
2. Luo, N.; Vidal, Y.; Acho, L. (Eds.) *Wind Turbine Control and Monitoring*, 2014 ed.; Advances in Industrial Control; Springer: Berlin, Germany, 2014; ISBN 9783319084121.
3. Odgaard, P.F.; Stoustrup, J. A Benchmark Evaluation of Fault Tolerant Wind Turbine Control Concepts. *IEEE Trans. Control Syst. Technol.* **2015**, *23*, 1221–1228.
4. Zhao, W.; Stol, K. Individual Blade Pitch for Active Yaw Control of a Horizontal—Axis Wind Turbine. In Proceedings of the 45th AIAA Aerospace Sciences Meeting and Exhibit, Reno, NV, USA, 8–11 January 2007.
5. Juditsky, A.; Hjalmarsson, H.; Beneviste, A.; Delyon, B.; Ljung, L.; Sjöberg, J.; Zhang, Q. Nonlinear Black-Box Modeling in System Identification: A Mathematical Foundation. *Automatica* **1995**, *31*, 1691–1724.
6. Babuška, R. *Fuzzy Modeling for Control*; Kluwer Academic Publishers: Boston, MA, USA, 1998.
7. Simani, S.; Fantuzzi, C.; Rovatti, R.; Beghelli, S. Parameter Identification for Piecewise Linear Fuzzy Models in Noisy Environment. *Int. J. Approx. Reason.* **1999**, *1*, 149–167.
8. Galdi, V.; Piccolo, A.; Siano, P. Designing an Adaptive Fuzzy Controller for Maximum Wind Energy Extraction. *IEEE Trans. Energy Convers.* **2008**, *23*, 559–569.
9. Simani, S.; Castaldi, P. Data-Driven and Adaptive Control Applications to a Wind Turbine Benchmark Model. *Control Eng. Pract.* **2013**, *21*, 1678–1693, doi:10.1016/j.conengprac.2013.08.009.
10. Landau, Y. *Adaptive Control*; Marcel Dekker: New York, NY, USA, 1979; ISBN 0-8247-6548-6.
11. Slotine, J.E.; Li, W. *Applied Nonlinear Control*; Prentice-Hall: Prentice Hall, NJ, USA, 1991.
12. Van Huffel, S.; Lemmerling, P. (Eds.) *Total Least Squares and Errors-in-Variables Modeling: Analysis, Algorithms and Applications*, 1st ed.; Springer: London, UK, 2002; ISBN 1402004761.
13. Ljung, L. *System Identification: Theory for the User*, 2nd ed.; Prentice Hall: Englewood Cliffs, NJ, USA, 1999.
14. Åström, K.J.; Hägglund, T. *Advanced PID Control*; ISA—The Instrumentation, Systems, and Automation Society: Research Triangle Park, NC, USA, 2006; ISBN 978-1-55617-942-6.
15. Van Engelen, T.; Schuurmans, J.; Kanev, S.; Dong, J.; Verhaegen, M.; Hayashi, Y. Fault tolerant wind turbine production operation and shutdown (Sustainable Control). In Proceedings of the EWEA, Brussels, Belgium, 14–17 March 2011.
16. Wei, X.; Verhaegen, M.; van den Engelen, T. Sensor fault diagnosis of wind turbines for fault tolerant. *IFAC Proc. Vol.* **2008**, 41, 3222–3227.
17. Dobrila, C.; Stefansen, R. Fault Tolerant Wind Turbine Control. Master's Thesis, Technical University of Denmark, Kgl, Denmark, 2007.
18. Odgaard, P.F.; Damgaard, C.; Nielsen, R. On-Line Estimation of Wind Turbine Power Coefficients Using Unknown Input Observers. *IFAC Proc. Vol.* **2008**, 41, 10646–10651.
19. Poure, P.; Weber, P.; Theilliol, D.; Saadate, S. Fault-tolerant power electronic converters: Reliability analysis of active power filter. In Proceedings of the IEEE International Symposium on Industrial Electronics ISIE, Vigo, Spain, 4–7 June 2007; pp. 3174–3179.
20. Rothenhagen, K.; Fuchs, F.W. Current sensor fault detection and reconfiguration for a doubly fed induction generator. In Proceedings of the IEEE Power Electronics Specialists Conference, Orlando, FL, USA, 17–21 June 2007; pp. 2732–2738.
21. Rothenhagen, K.; Fuchs, F.W. Doubly Fed Induction Generator Model-Based Sensor Fault Detection and Control Loop Reconfiguration. *IEEE Trans. Ind. Electron.* **2009**, *56*, 4229–4238.
22. Odgaard, P.F.; Stoustrup, J.; Kinnaert, M. Fault Tolerant Control of Wind Turbines—A Benchmark Model. *IFAC Proc. Vol.* **2009**, 1, 155–160.
23. Esbensen, T.; Sloth, C. *Fault Diagnosis and Fault Tolerant Control of Wind Turbines*; Department of Electronic Systems, Aalborg University: Aalborg, Denmark, 2008.
24. Esbensen, T.; Sloth, C.; Odgaard Niss, M.; Thorarins Jensen, B. *Fault Diagnosis and Fault Tolerant Control of Wind Turbines*; Department of Electronic Systems, Aalborg University: Aalborg, Denmark, 2009.
25. Odgaard, P.F.; Stoustrup, J.; Kinnaert, M. Fault-Tolerant Control of Wind Turbines: A Benchmark Model. *IEEE Trans. Control Syst. Technol.* **2013**, *21*, 1168–1182, doi:10.1109/TCST.2013.2259235.

26. Schulte, H.; Georg, S. Nonlinear Control of Wind Turbines with Hydrostatic Transmission Based on Takagi–Sugeno Model. *J. Phys. Conf. Ser.* **2014**, *524*, 1–8, doi:10.1088/1742-6596/524/1/012085.
27. Zhao, M.; Ji, J.C. Nonlinear torsional vibrations of a wind turbine gearbox. *Appl. Math. Model.* **2015**, *39*, 4928–4950, doi:10.1016/j.apm.2015.03.026.
28. Zhao, M.; Ji, J.C. Dynamic Analysis of Wind Turbine Gearbox Components. *Energies* **2016**, *9*, 110, doi:10.3390/en9020110.
29. Simani, S. Application of a Data-Driven Fuzzy Control Design to a Wind Turbine Benchmark Model. *Adv. Fuzzy Syst.* **2012**, *2012*, 1–12, doi:10.1155/2012/504368.
30. Rovatti, R.; Fantuzzi, C.; Simani, S. High-speed DSP-based implementation of piecewise-affine and piecewise-quadratic fuzzy systems. *Signal Process.* **2000**, *80*, 951–963, doi:10.1016/S0165-1684(00)00013-X.
31. Sun, F.; Sun, Z.; Li, L.; Li, H.X. Neuro-fuzzy adaptive control based on dynamic inversion for robotic manipulators. *Fuzzy Sets Syst.* **2003**, *134*, 117–133, doi:10.1016/S0165-0114(02)00233-6.
32. Machácek, J.; Bobál, V. Adaptive PID controller with on-line identification. *J. Electr. Eng.* **2002**, *53*, 233–240.
33. Bobál, V.; Chalupa, P. *Self-Tuning Controllers Simulink Library*; Tomas Bata University in Zlín, Faculty of Technology: Zlín, Czech, 2002. Avaialble online: http://www.utb.cz/stctool/ (accessed on 24 November 2017).
34. Cheong, S.Y.; Safonov, M.G. Bumpless transfer for adaptive switching controls. *IFAC Proc. Vol.* **2008**, 41, 14415–14420.
35. Jun, M.; Safonov, M.G. Automatic PID tuning: An application of unfalsified control. In Proceedings of the IEEE International Symposium on Computer Aided Control System Design, Kohala Coast, HI, USA, 27 August 1999; pp. 328–333.
36. Skogestad, S. Simple analytic rules for model reduction and PID controller tuning. *J. Process Control* **2003**, *13*, 291–309, doi:10.1016/S0959-1524(02)00062-8.
37. Johnson, K.E.; Pao, L.Y.; Balas, M.J.; Kulkarni, V.; Fingersh, L.J. Stability analysis of an adaptive torque controller for variable speed wind turbines. In Proceedings of the 43rd IEEE Conference on Decision and Control, Nassau, Bahamas, 14–17 December 2004; Volume 4, pp. 4087–4094.
38. Chen, J.; Patton, R.J. *Robust Model-Based Fault Diagnosis for Dynamic Systems*; Kluwer Academic Publishers: Boston, MA, USA, 1999.
39. Zhang, Y.; Jiang, J. Bibliographical review on reconfigurable fault-tolerant control systems. *Annu. Rev. Control* **2008**, *32*, 229–252.
40. Patton, R.J.; Uppal, F.J.; Simani, S.; Polle, B. Robust Fdi Applied to Thruster Faults of a Satellite System. *Control Eng. Pract.* **2010**, *18*, 1093–1109, doi:10.1016/j.conengprac.2009.04.011.
41. Ho, W.K.; Xu, W. PID tuning for unstable processes based on gain and phase-margin specifications. *IEE Proc. Control Theory Appl.* **1998**, *145*, 392–396, doi:10.1049/ip-cta:19982243.
42. Laouti, N.; Sheibat-Othman, N.; Othman, S. Support vector machines for fault detection in wind turbines. *IFAC Proc. Vol.* **2011**, 18, 7067–7072, doi:10.3182/20110828-6-IT-1002.02560.
43. Zhang, X.; Zhang, Q.; Zhao, S.; Ferrari, R.M.G.; Polycarpou, M.M.; Parisini, T. Fault detection and isolation of the wind turbine benchmark: An estimation-based approach. *IFAC Proc. Vol.* **2011**, 18, 8295–8300, doi:10.3182/20110828-6-IT-1002.02808.
44. Ozdemir, A.A.; Seiler, P.; Balas, G.J. Wind turbine fault detection using counter-based residual threshold-ing. *IFAC Proc. Vol.* **2011**, 18, 8289–8294, doi:10.3182/20110828-6-IT-1002.01758.
45. Chen, W.; Ding, S.X.; Sari, A.H.A.; Naik, A.; Khan, A.Q.; Yin, S. Observer-based FDI schemes for wind turbine benchmark. *IFAC Proc. Vol.* **2011**, 18, 7073–7078, doi:10.3182/20110828-6-IT-1002.03469.
46. Svard, C.; Nyberg, M. Automated design of an FDI system for the wind turbine benchmark. *IFAC Proc. Vol.* **2011**, 18, 8307–8315, doi:10.3182/20110828-6-IT-1002.00618.
47. Simani, S.; Castaldi, P. Adaptive Fault-Tolerant Control Design Approach for a Wind Turbine Benchmark. *IFAC Proc. Vol.* **2012**, 8, 319–324, doi:10.3182/20120829-3-MX-2028.00066.
48. Shi, F.; Patton, R.J. An active fault tolerant control approach to an offshore wind turbine Model. *Renew. Energy* **2015**, *75*, 788–798, doi:10.1016/j.renene.2014.10.061.
49. Towers, P.D.; Jones, B.L. Real-time wind field reconstruction from LiDAR measurements using a dynamic wind model and state estimation. *Wind Energy* **2014**, *19*, 133–150, doi:10.1002/we.1824.

50. Odgaard, P.F.; Johnson, K. Wind Turbine Fault Diagnosis and Fault Tolerant Control—An Enhanced Benchmark Challenge. In Proceedings of the 2013 American Control Conference, Washington, DC, USA, 17–19 June 2013; pp. 4447–4452.
51. Fischer, T.; de Vries, W.; Rainey, P.; Schmidt, B.; Argyriadis, K.; Kühn, M. Offshore support structure optimization by means of integrated design and controls. *Wind Energy J.* **2012**, *15*, 99–117.

© 2017 by the authors. Licensee MDPI, Basel, Switzerland. This article is an open access article distributed under the terms and conditions of the Creative Commons Attribution (CC BY) license (http://creativecommons.org/licenses/by/4.0/).